Midpoint Regularization: from High Uncertainty Training to Conservative Classification

Hongyu Guo

National Research Council Canada
1200 Montreal Road, Ottawa, Ontario, K1A 0R6
hongyu.guo@nrc-cnrc.gc.ca

Abstract. Label Smoothing (LS) improves model generalization through penalizing models from generating overconfident output distributions. For each training sample the LS strategy smooths the one-hot encoded training signal by distributing its distribution mass over the non-ground truth classes. We extend this technique by considering example pairs, coined PLS. PLS first creates midpoint samples by averaging random sample pairs and then learns a smoothing distribution during training for each of these midpoint samples, resulting in midpoints with high uncertainty labels for training. We empirically show that PLS significantly outperforms LS, achieving up to 30% of relative classification error reduction. We also visualize that PLS produces very low winning softmax scores for both in and out of distribution samples.

Keywords: Label Smoothing · Model Regularization · Mixup.

1 Introduction

Label Smoothing (LS) is a commonly used output distribution regularization technique to improve the generalization performance of deep learning models [4, 13, 15, 20, 21, 23, 30]. Instead of training with data associated with one-hot labels, models with label smoothing are trained on samples with soft targets, where each target is a weighted mixture of the ground truth one-hot label with the uniform distribution of the classes. This penalizes overconfident output distributions, resulting in improved model generalization [16, 18, 19, 26, 29].

When smoothing the one-hot training signal, existing LS methods, however, only consider the distance between the only gold label and the non-ground truth targets. This motivates our Pairwise Label Smoothing (PLS) strategy, which takes a pair of samples as input. In a nutshell, the PLS first creates a midpoint sample by averaging the inputs and labels of a sample pair, and then distributes the distribution mass of the two ground truth targets of the new midpoint sample over its non-ground truth classes. Smoothing with a pair of ground truth labels enables PLS to preserve the relative distance between the two truth labels while being able to further soften that between the truth labels and the other class targets. Also, unlike current LS methods, which typically require to find a global smoothing distribution mass through cross-validation search, PLS

Fig. 1. Average distribution mass (Y-axis) of PLS and Mixup (from sample pairs with different labels) and ULS on Cifar10's 10 classes (X-axis). PLS' class-wise training signals are spread out, with gold labels probabilities close to 0.35, which has larger uncertainty than that of 0.5 and 0.9 from Mixup and ULS, receptivity.

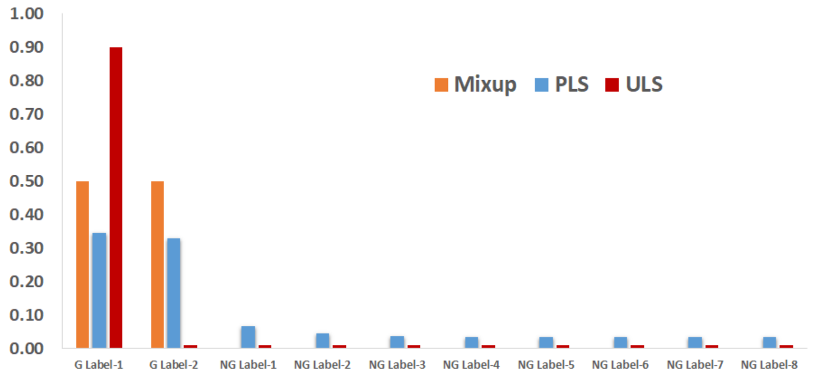

automatically learns the distribution mass for each input pair during training. Hence, it effectively eliminates the turning efforts for searching the right level of smoothing strength for different applications.

Also, smoothing with a pair of labels empowers PLS to be trained with low distribution mass (i.e., high uncertainty) for the ground truth targets. Figure 1 depicts the average values (over all the midpoint samples created from sample pairs with different labels) of the 10 target classes in Cifar10 used by PLS for training. These ground truth targets are smaller than 0.35, which represents much larger uncertain than the 0.5 and 0.9 in Mixup and the uniform label smoothing (denoted as ULS), respectively. Owing to such high uncertainty ground truth target training signals, PLS produces extremely low winning softmax scores during testing, resulting in very conservative classification decisions. Figure 2 depicts the histograms of the winning softmax scores of Mixup, ULS and PLS on the Cifar10 validation data. Unlike Mixup and ULS, PLS produced very conservative softmax scores, with extremely sparse distribution in the high confidence region. Such conservative classifications are produced not only on in-distribution data but also on out-of-distribution samples.

We empirically show that PLS significantly outperforms LS and Mixup [28], with up to 30% of relative classification error reduction. We also visualize that PLS produces extremely conservative predictions in testing time, with many of its winning predicted softmax scores slightly over 0.5 for both in and out of distribution samples.

2 Related Work

Label smoothing has shown to provide consistent model generalization gains across many tasks [21, 19, 24, 18, 16, 15]. Unlike the above methods which apply

Fig. 2. Histograms of the winning softmax scores on Cifar10 validation data, generated by ULS (right Y-axis) and by Mixup and PLS (left Y-axis) where the X-axis depicts the softmax score. The PLS produces very low softmax winning scores; the differences versus the ULS and Mixup are striking: the PLS models are extremely sparse in the high confidence region at the right end.

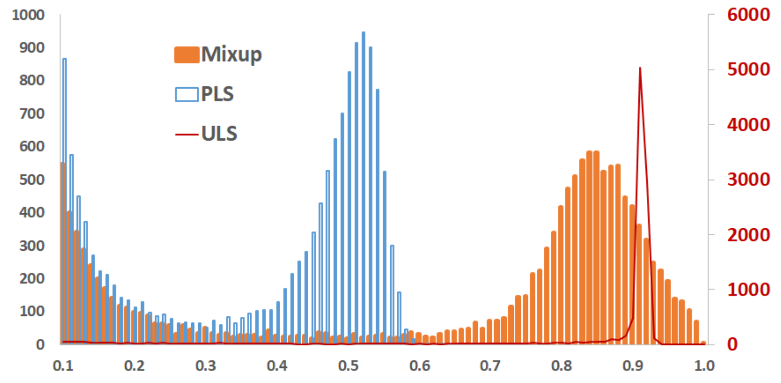

label smoothing to each single input, our smoothing strategy leverages a pair of inputs for label smoothing. Furthermore, unlike existing LS approaches which deploy one static and uniform smoothing distribution for all the training samples, our strategy automatically learns a dynamic distribution mass for each sample during training.

Mixup methods [2, 8–10, 22, 27, 28] create *a large number* of synthetic samples with various features from a sample pair, through interpolating the pair's both features and labels with mixing coefficients randomly sampling between [0,1]. In contrast, our approach creates *only the midpoint* sample of a sample pair (equivalent to Mixup with a fixed mixing ratio of 0.5). More importantly, our method adds a label smoothing component on the midpoint samples. That is, we adaptively learn a distribution mass to smooth the pair of ground truth labels of each midpoint sample, with the aims of deploying high uncertainty training targets (much higher than that of Mixup) for output distribution regularization. Such high uncertain training labels result in PLS producing very conservative classification decisions and superior accuracy than Mixup.

The generation of the smoothing distribution in our method is also related to self-distillation [1, 6, 12, 17, 25]. However, these approaches treat the final predictions as target labels for a new round of training, and the teacher and student architectures are identical [17]. In our method, the classification and the smoothing distribution generator have different network architectures, and the training targets for the classification are a mixture of the outputs of the two networks.

3 Label Smoothing over Midpoint Samples

Our proposed method PLS leverages a pair of samples, randomly selected from the training data set, to conduct label smoothing. It first creates a midpoint sample for each sample pair, and then adaptively learns a smoothing distribution for each midpoint sample. These midpoint samples are then used for training to regularize the learning of the networks.

3.1 Preliminaries

We consider a standard classification setting with a given training data set $(X;Y)$ associated with K candidate classes $\{1, 2, \cdots, K\}$. For an example x_i from the training dataset $(X;Y)$, we denote the ground truth distribution q over the labels as $q(y|x_i)$ ($\sum_{y=1}^{K} q(y|x_i) = 1$). Also, we denote a neural network model to be trained as f_θ (parameterized with θ), and it produces a conditional label distribution over the K classes as $p_\theta(y|x_i)$:

$$p_\theta(y|x_i) = \frac{\exp(z_y)}{\sum_{k=1}^{K} \exp(z_{y_k})}, \tag{1}$$

with $\sum_{y=1}^{K} p_\theta(y|x_i) = 1$, and z is noted as the logit of the model f_θ. The logits are generated with two steps: the model f_θ first constructs the m-dimensional input embedding $S_i \in R^m$ for the given input x_i, and then passes it through a linear fully connected layer $W_l \in R^{K \times m}$:

$$S_i = f_\theta(x_i), z = W_l S_i. \tag{2}$$

During learning, the model f_θ is trained to optimize the parameter θ using the n examples from $(X;Y)$ by minimizing the cross-entropy loss:

$$\ell = -\sum_{i=1}^{n} H_i(q, p_\theta). \tag{3}$$

Instead of using one-hot encoded vector for each example x_i in $(X;Y)$, label smoothing (LS) adds a smoothed label distribution (i.e., the prior distribution) $u(y|x_i)$ to each example x_i, forming a new target label, namely soft label:

$$q'(y|x_i) = (1-\alpha) q(y|x_i) + \alpha u(y|x_i), \tag{4}$$

where hyper-parameter α is a weight factor ($\alpha \in [0, 1]$) needed to be tuned to indicate the smoothing strength for the one-hot label. This modification results in a new loss:

$$\ell' = -\sum_{i=1}^{n} \Big[(1-\alpha) H_i(q, p_\theta) + \alpha H_i(u, p_\theta)\Big]. \tag{5}$$

Usually, the $u(y|x_i)$ is a uniform distribution, independent of data x_i, as $u(y|x_i) = 1/K$, and hyper-parameter α is tuned with cross-validation.

3.2 Midpoint Generation

For a sample, denoted as x_i, from the provided training set $(X; Y)$ for training, PLS first randomly selects [1] another training sample x_j. For the pair of samples $(x_i; y_i)$ and $(x_j; y_j)$, where x is the input and y the one-hot encoding of the corresponding class, PLS then generates a synthetic sample through element-wisely averaging both the input features and the labels, respectively, as follows:

$$x_{ij} = (x_i + x_j)/2, \tag{6}$$

$$q(y|x_{ij}) = (y_i + y_j)/2. \tag{7}$$

These synthetic samples can be considered as the *midpoint samples* of the original sample pairs. It is also worth noting that, the midpoint samples here are equivalent to fixing the linear interpolation mixing ratios as 0.5 in the Mixup [28] method. Doing so, for the midpoint sample x_{ij} we have the ground truth distribution q over the labels as $q(y|x_{ij})$ ($\sum_{y=1}^{K} q(y|x_{ij}) = 1$). The newly resulting midpoint x_{ij} will then be used for label smoothing (will be discussed in detail in Section 3.3) before feeding into the networks for training. In other words, the predicted logits as defined in Equation 2 is computed by first generating the m-dimensional input embedding $S_{ij} \in R^m$ for x_{ij} and then passing through the fully connected linear layer to construct the logit z:

$$S_{ij} = f_\theta(x_{ij}), \tag{8}$$

$$z = W_l S_{ij}. \tag{9}$$

Hence, the predicted conditional label distribution over the K classes produced by the networks is as follows:

$$p_\theta(y|x_{ij}) = \frac{\exp(z_y)}{\sum_{k=1}^{K} \exp(z_{y_k})}. \tag{10}$$

3.3 Learning Smoothing Distribution for Midpoints

PLS leverages a learned distribution, which depends on the input x, to dynamically generate the smoothing distribution mass for midpoint samples to distribute their ground truth target distribution to the non-target classes. To this end, the PLS implements this by adding a fully connected layer to the network f_θ. That is, the f_θ produces two projections from the *penultimate* layer representations of the network: one for the logits as the original network (Equation 9), and another for generating the smoothing distribution as follows.

In specific, an additional fully connected layer $W_t \in R^{K\times m}$ is added to the original networks f_θ to produce the smoothing distribution over the K classification classes. That is, for the given input image x_{ij}, its smoothing distributions

[1] For efficiency purpose, we implement this by randomly selecting a sample from the same mini-batch during training.

over the K classification targets, denoted as $u'_\theta(y|x_{ij})$, are computed as follows:

$$u'_\theta(y|x_{ij}) = \frac{\exp(v_y)}{\sum_{k=1}^{K} \exp(v_{y_k})}, \tag{11}$$

$$v = \sigma(W_t S_{ij}), \tag{12}$$

where σ denotes the Sigmoid function, and S_{ij} is the same input embedding as that in Equation 9. In other words, the two predictions (i.e., Equations 9 and 12) share the same networks except the last fully connected layer. That is, the only difference between PLS and the original networks is the added fully connected layer W_t. The added Sigmoid function here aims to squash the smoothing distributions learned for different targets to the same range of [0, 1].

After having the smoothing distributions $u'_\theta(y|x_{ij})$, PLS then uses them to smooth the ground truth labels $q(y|x_{ij})$ as described in Equation 7, with average:

$$q'(y|x_{ij}) = (q(y|x_{ij}) + u'_\theta(y|x_{ij}))/2. \tag{13}$$

The loss function of PLS thus becomes the follows:

$$\ell' = -\sum_{i=1}^{n} \Big[0.5 \cdot H_i(q(y|x_{ij}), p_\theta(y|x_{ij})) + 0.5 \cdot H_i(u'_\theta(y|x_{ij}), p_\theta(y|x_{ij})) \Big]. \tag{14}$$

Coefficient 0.5 here helps prevent the network from over-distributing its label distribution to the non-ground truth targets. Over-smoothing degrades the model performance, as will be shown in the experiments. Also, 0.5 here causes the resulting training signals to have high uncertainty regarding the ground truth targets. Such high uncertainty helps train the models to make conservative predictions.

3.4 Optimization

For training, PLS minimizes, with gradient descent on mini-batch, the loss ℓ'. One more issue needs to be addressed for the training. That is, the midpoint samples used for training, namely $(x_{ij}; y)$, may lack information on the original training samples $(x_i; y)$ due to the average operation in midpoint generation. To compensate this, we alternatively feed inputs to the networks with either a mini-batch from the original inputs, i.e., x_i or x_{ii}, or a mini-batch from the midpoint samples, i.e., x_{ij}. Note that, when training with the former, the networks still need to learn to assign the smoothing distribution $u'_\theta(y|x_{ii})$ to form the soft targets $q'(y|x_{ii})$ for the sample x_{ii}. As will be shown in the experiment section, this training strategy is important to PLS' regularization effect.

4 Experiments

We first show our method's superior accuracy, and then visualize its high uncertainty training labels and conservative classifications.

Methods	MNIST	Fashion	SVHN	Cifar10	Cifar100	Tiny-ImageNet
PreAct ResNet-18	0.62 ±0.05	4.78±0.19	3.64± 0.42	5.19±0.30	24.19± 1.27	39.71±0.08
ULS-0.1	0.63±0.02	4.81±0.07	3.20 ±0.06	4.95±0.15	21.62±0.29	38.85±0.56
ULS-0.2	0.62±0.02	4.57±0.05	3.14±0.11	4.89±0.11	21.51±0.25	38.54±0.32
ULS-0.3	0.60±0.01	4.60±0.06	3.12±0.03	5.02±0.12	21.64±0.27	38.32±0.37
Mixup	0.56±0.01	4.18± 0.02	3.37±0.49	3.88± 0.32	21.10±0.21	38.06±0.29
Mixup-ULS0.1	0.53±0.02	4.13±0.10	2.96±0.39	4.00±0.17	21.51±0.51	37.23±0.48
Mixup-ULS0.2	0.53±0.03	4.18±0.09	3.02±0.42	3.95±0.13	21.41±0.55	38.21±0.38
Mixup-ULS0.3	0.50±0.02	4.15±0.06	2.88±0.31	4.06±0.04	20.94±0.49	38.93±0.43
PLS	**0.47 ±0.03**	**3.96±0.05**	**2.68 ±0.09**	**3.63±0.10**	**19.14±0.20**	**35.26±0.10**

Table 1. Error rate (%) of the testing methods with PreAct ResNet-18 [11] as baseline. We report mean scores over 5 runs with standard deviations (denoted ±). Best results are in **Bold**.

Methods	MNIST	Fashion	SVHN	Cifar10	Cifar100	Tiny-ImageNet
ResNet-50	0.61±0.05	4.55±0.14	3.22±0.05	4.83±0.30	23.10±0.62	35.67±0.50
ULS-0.1	0.63±0.02	4.58±0.16	2.98±0.02	4.98±0.25	23.90±0.99	35.02±0.39
ULS-0.2	0.62±0.03	4.52±0.04	3.08±0.03	5.00±0.35	23.88±0.73	36.19±0.66
ULS-0.3	0.65±0.03	4.51±0.15	3.04±0.07	5.16±0.16	23.17±0.50	36.14±0.06
Mixup	0.57± 0.03	4.31±0.05	2.85±0.07	4.29±0.28	19.48±0.48	32.36±0.53
Mixup-ULS0.1	0.60±0.04	4.28±0.12	2.90±0.09	4.02±0.27	21.58±0.86	32.11±0.09
Mixup-ULS0.2	0.58±0.02	4.33±0.09	2.89±0.07	4.09±0.10	20.87±0.51	32.81±0.48
Mixup-ULS0.3	0.57±0.04	4.29±0.11	2.84±0.10	4.19±0.18	21.64±0.41	33.94±0.56
PLS	**0.51± 0.02**	**4.15±0.09**	**2.36±0.03**	**3.60±0.18**	**18.65±1.08**	**30.73±0.20**

Table 2. Error rate (%) of the testing methods with ResNet-50 [11] as baseline. We report mean scores over 5 runs with standard deviations (denoted ±). Best results are in **Bold**.

4.1 Datasets, Baselines, and Settings

We use six benchmark image classification tasks. **MNIST** is a digit (1-10) recognition dataset with 60,000 training and 10,000 test 28x28-dimensional gray-level images. **Fashion** is an image recognition dataset with the same scale as MNIST, containing 10 classes of fashion product pictures. **SVHN** is the Google street view house numbers recognition data set. It has 73,257 digits, 32x32 color images for training, 26,032 for testing, and 531,131 additional, easier samples. Following literature, we did not use the additional images. **Cifar10** is an image classification task with 10 classes, 50,000 training and 10,000 test samples. **Cifar100** is similar to Cifar10 but with 100 classes and 600 images each. **Tiny-ImageNet** [5] has 200 classes, each with 500 training and 50 test 64x64x3 images.

We conduct experiments using the popular benchmarking networks PreAct ResNet-18 and ResNet-50 [11]. We compare with the label smoothing methods [18, 16] (denoted as ULS) with various smoothing coefficients (i.e., α in Equation 5), where ULS-0.1, ULS-0.2, and ULS-0.3 denote the smoothing coefficient of 0.1, 0.2, and 0.3, respectively. We also compare with the input-pair based data augmentation method Mixup [28]. We further compare with methods that stacking the ULS on top of Mixup, denoted Mixup-ULS0.1, Mixup-ULS0.2, and Mixup-ULS0.3.

For Mixup, we use the authors' code at [2] and the uniformly selected mixing coefficients between [0,1]. For PreAct ResNet-18 and ResNet-50, we use the implementation from Facebook [3]. For PLS, the added fully connected layer is the same as the last fully connected layer of the baseline network with a Sigmoid function on the top. All models are trained using mini-batched (128 examples) backprop, with the *exact settings* as in the Facebook codes, for 400 epochs. Each reported value (accuracy or error rate) is the mean of five runs on a NVIDIA GTX TitanX GPU with 12GB memory.

4.2 Predictive Accuracy

The error rates obtained by ULS, Mixup, Mixup-ULS, and PLS using ResNet-18 as baseline on the six test datasets are presented in Table 1. The results with ResNet-50 as baselines are provided in Table 2.

Table 1 shows that PLS outperforms, in terms of predictive error, the ResNet-18, the label smoothing models (ULS-0.1, ULS-0.2, ULS-0.3), Mixup, stacking ULS on top of Mixup (Mixup-ULS0.1, Mixup-ULS0.2, Mixup-ULS0.3) on all the six datasets. For example, the relative improvement of PLS over ResNet-18 on Cifar10 and MNIST are over 30% and 24%, respectively. When considering PLS and the average error obtained by the three ULS models, on both Cifar10 and MNIST, the relative improvement is over 23%. It is also promising to see that on Tiny-ImageNet, PLS reduced the absolute error rates over Mixup, Mixup-ULS, and ULS from about 38% to 35%.

For the cases with ResNet-50 as baselines, Table 2 indicates that similar error reductions are obtained by PLS. Again, on all the testing datasets, PLS outperforms all the comparison baselines. For example, for Cifar10, the relative improvement achieved by PLS over ResNet-50 and the average of the three label smoothing strategies (i.e. ULS) are 25.47% and 28.67%, respectively. For Cifar100 and Tiny-ImageNet, PLS reduced the absolute error rates of ULS from 23% and 36% to 18.65% and 30.73% respectively.

An important observation here is that, stacking label smoothing on top of Mixup (i.e., Mixup-ULS) did not improve, or even degraded, Mixup's accuracy. For example, for Cifar10, Cifar100, and Tiny-ImageNet (the last three columns in Tables 1 and 2), Mixup-ULS obtained similar or slightly higher error rate than Mixup. The reason here is that Mixup creates samples with soft labels through linearly interpolating between [0, 1], which is a form of label smoothing regularization [3]. Consequently, stacking another label smoothing regularizer on top of Mixup can easily mess up the soft training targets, resulting in underfitting. Promisingly, PLS was able to improve over Mixup and Mixup-ULS. For example, on Tiny-ImageNet PLS outperformed Mixup and Mixup-ULS by reducing the error from 38.06% to 35.26% and from 32.36% to 30.73%, respectively, when using ResNet-18 and ResNet-50. Similar error reduction can be observed on Cifar10 and Cifar100.

[2] https://github.com/facebookresearch/mixup-cifar10

[3] https://github.com/facebookresearch/mixup-cifar10/models/

4.3 Ablation Studies

Impact of Learned Distribution and Original Samples We evaluate the impact of the key components in PLS using ResNet-18 and ResNet-50 on Cifar100. Results are in Table 3. The key components include 1) removing the learned smoothing distribution mass in Equation 13, 2) excluding the original training inputs as discussed in the method section, and 3) replacing the learned smoothing distribution mass with uniform distribution with weight coefficients of 0.1, 0.2, and 0.3 (denoted UD-0.1, UD-0.2 and UD-0.3).

The error rates obtained in Table 3 show that, both the learned smoothing distribution and the original training samples are critical for PLS. In particular, when excluding the original samples from training, the predictive error of PLS dramatically increased from about 19% to nearly 24% for both ResNet-18 and ResNet-50. The reason, as discussed in the method section, is that, without the original training samples, the networks are trained with midpoint samples only, thus may lack information on the validation samples with one-hot labels.

PLS	ResNet-18	ResNet-50
	19.14	18.65
—- no learned distribution	21.06	19.35
—- no original samples	23.84	24.42
—- UD 0.1	19.50	18.91
—- UD 0.2	19.25	18.81
—- UD 0.3	19.31	18.89

Table 3. Error rates (%) on Cifar100 by PLS while varying its key components: no learned distribution, no original samples, replacing learned smoothing distribution with uniform distribution.

Also, Table 3 indicates that, replacing the learned smoothing distribution in PLS with manually tuned Uniform distribution (i.e., UD) obtained slightly larger errors. This indicates that PLS is able to learn the distribution to smooth the two target labels in the midpoint samples, resulting in superior accuracy and excluding the need for the coefficient search for different applications.

Learning Smoothing Coefficient We also conducted experiments of learning the smoothing coefficient, instead of learning the smoothing distribution, for each midpoint example. That is, we replace Equation 12 with $\sigma(W_t S_{ij})$ where W_t is $R^{1\times m}$ instead of $R^{K\times m}$. Table 4 presents the error rates (%) obtained using PreAct ResNet-18 and ResNet-50 on Cifar100 and Cifar10. These results suggest that learning to predict smoothing distribution significantly better than predicting the smoothing coefficient in PLS.

Re-weight Smoothing Strength PLS distributes half of a midpoint sample's ground truth distribution mass over the non-ground truth targets (Equation 13). We here evaluate the impact of different weight factors between the ground truth and non-ground truth targets, by varying it from 0.1 to 0.9 (0.5

PLS	ResNet-18	ResNet-50
	pred. coeff. / PLS	pred. coeff. / PLS
Cifar100	21.60 / 19.14	19.21 / 18.65
Cifar10	4.67 / 3.63	4.06 / 3.60

Table 4. Error rates (%) on Cifar100 and Cifar10 obtained by PLS while predicting the smoothing coefficient (pred. coeff.) instead of learning the smoothing distribution (PLS) for each sample pair.

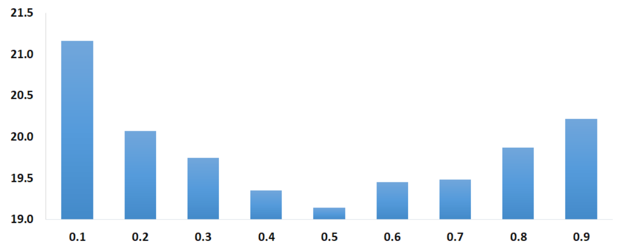

Fig. 3. Error rates (%, Y-axis) on Cifar100 obtained by varying the weight factor in PLS from 0.1 to 0.9 (X-axis).

equals to the average used by PLS). The results obtained by PLS using ResNet-18 on Cifar100 are in Figure 3. The error rates in Figure 3 suggest that average used by midpoints in PLS provides better accuracy than other weighting ratios. This is expected as discussed in Section 3.3.

4.4 Uncertainty Label and Conservative Classification

This section will show that PLS utilizes high uncertainty labels from midpoint samples for training and produces very conservative classification decisions in testing.

High Uncertainty Labels in Training We visualize, in Figure 4, the soft target labels used for training by PLS with ResNet-18 on Cifar100 (top) and Cifar10 (bottom). Figure 4 depicts the soft label values of the training samples for both the ground truth targets (in green) and their top 5 largest non-ground truth classes (in orange). The figure presents the average values over all the training samples resulting from sample pairs with two different one-hot true labels. Here, X-axis depicts the training targets, and Y-axis the corresponding distribution mass.

Results in Figure 4 indicate that, PLS uses much smaller target values for the ground truth labels during training, when compared to the one-hot representation label used by the baselines and the soft targets used by label smoothing ULS and Mixup. For example, the largest ground truth targets for PLS are around 0.25 and 0.35 (green bars), respectively, for Cifar100 and Cifar10. These values are much smaller than 1.0 used by the baselines and 0.9 and 0.5 used by ULS-0.1 and Mixup respectively. Consequently, in PLS, the distance between the ground truth targets and the non-ground truth targets are much smaller than that in the baseline, ULS-0.1 and Mixup. In addition, the distance between the two ground truth targets in PLS (green bars) is very small, when compared to the distance between the ground truth and non-ground truth target values (green vs. orange bars).

Fig. 4. Average distribution of ground truth targets (green bars) and the top 5 largest non-ground truth targets (orange bars) used by PLS in training with ResNet-18 on Cifar100 (top) and Cifar10 (bottom). X-axis is the classes and Y-axis the distribution mass.

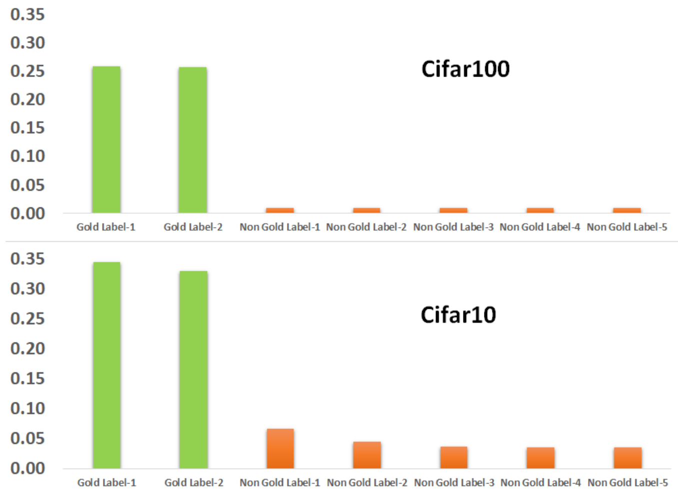

These results indicate that the training samples in PLS have smoother training targets across classes, and those training signals are far from 1.0 (thus with much higher uncertainty), which in turn impacts how PLS makes its classification decisions as will be discussed next.

Low Predicted Softmax Scores in Testing One effect of the high uncertainty training signals (far from 1.0) as discussed above was reflected on the model's prediction scores made in test time. Figure 5 visualizes the predicted winning softmax scores made by ResNet-18 (top row), ULS-0.1 (second row), Mixup (third row) and PLS (bottom row) on all the 10K test data samples in Cifar100 (left column) and Cifar10 (right column). To have better visualization, we have removed the predictive scores less than 0.1 for all the methods since all models obtained similar results for confidences smaller than 0.1.

For Cifar100, results on the left of Figure 5 indicate that ResNet-18 produced very confident predictions (top-left subfigure), namely skewing large mass of its predicted softmax scores on 1.0 (i.e., 100% confidence). On the other hand, ULS and Mixup were able to decrease its prediction confidence at test time (middle rows/left). They spread their predictive confidences to the two ends, namely moving most of the predicted scores into two bins [0.1-0.2] and [0.8-1.0]. In contrast, PLS produced very conservative predicted softmax scores, by distributing many of its predicted scores to the middle, namely 0.5, and with sparse distribution for scores larger than 0.7 (bottom left subfigure).

For Cifar10, results on the right of Figure 5 again indicate that ResNet-18 (top) produced very confident predictions, putting large mass of its predicted softmax scores near 1.0. For ULS and Mixup (middle rows), the predicted softmax scores were also distributed near the 1.0, but they are much less than that of ResNet-18. In contrast, PLS (bottom right) again generated very conservative predicted softmax scores. Most of them distributes near the middle of the softmax score range, namely 0.5, with a very few larger than 0.6.

These results suggest that, resulting from high uncertainty training signals across classes, PLS becomes extremely conservative when generating predicted scores in test time, producing low winning softmax scores for classification.

Impact on Model Calibration The conservative predictions generated by PLS improve the model's accuracy, but how such low softmax scores affect the calibration of the output probabilities? In this section, we report the Expected Calibration Error (ECE) [7] obtained by the baseline PreAct ResNet-18, ULS-0.1, Mixup and PLS on the test set with 15 bins as used in [18] for both Cifar100 and Cifar10.

Results in Figure 6 indicate that ULS (dark curve) is able to reduce the miscalibration error ECE on the Cifar100 data set (left subfigure), but for the Cifar10 dataset (right subfigure), ULS has larger ECE error after 100 epochs of training than the baseline model. Also, Mixup has higher ECE error than ULS on both Cifar100 and Cifar10. However, the ECE errors obtained by the PLS methods for both the Cifar100 and Cifar10 are much larger than the baseline, ULS and Mixup. Note that, although the authors in [7] state that the Batch Normalization (BN) strategy [14] also increases the miscalibration ECE errors for unknown reasons, we doubt that the PLS will have the same reason as the BN approach. This is because the main characteristic of the PLS model is that it produces extremely conservative winning softmax scores which is not the case for the BN strategy. We here suspect that the high ECE score of the PLS method may be caused by the fact that ECE is an evenly spaced binning metrics but the PLS produces sparse dispersion of the softmax scores across the range.

To verify the above hypothesis, we further investigate the Temperature Scaling (TS) method [7], which enables redistributing the distribution dispersion after training with no impact on the testing accuracy. During testing, TS multiplies the logits by a scalar before applying the softmax operator. We apply this TS technique to PLS, and present the results in Figure 6, depicting by red curve in the left and right subfigures for the Cifar100 and Cifar10, respectively. The TS factors was 0.5 and 0.2 respectively for Cifar100 and Cifar10, which were found

Fig. 5. Histograms of predicted softmax scores on the validation data by ResNet-18 (top row), ULS-0.1 (second row), Mixup (third row), and PLS (bottom row) on Cifar100 (left) and Cifar10 (right).

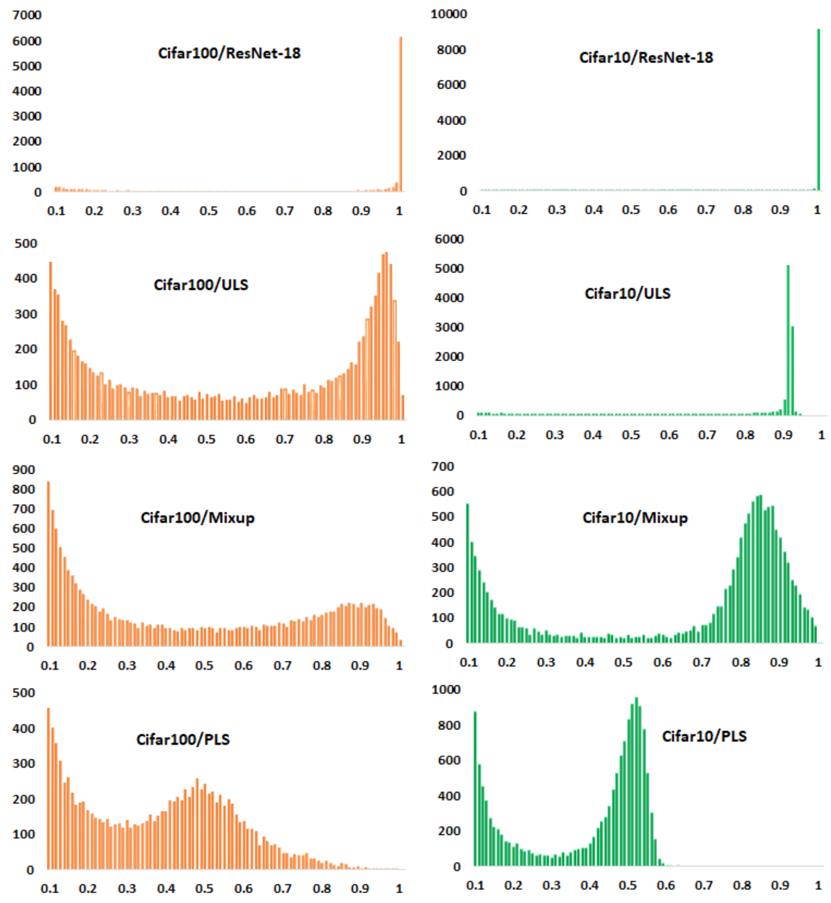

by a search with 10 percentage of the training data. Figure 6 indicates that TS can significantly improve the calibration of PLS for both cases. The ECE errors obtained by PLS-TS for both Cifar100 and Cifar10 (red curves) are lower than that of the baseline, ULS, and Mixup.

4.5 Testing on Out-of-Distribution Data

Section 4.4 shows that PLS produces very conservative classification decisions for in-distribution samples. We here explore the effect of PLS on out-of-distribution data.

In this experiment, we first train a ResNet-18 or ResNet-50 network (denoted as vanilla models) with in-distribution data (using either Cifar10 or Cifar100)

Fig. 6. ECE curves on the validation data of Cifar100 (left) and Cifar10 (right) from ResNet-18, ULS-0.1, Mixup, PLS and PLS with TS. X-axis is the training epoch and Y-axis the ECE value.

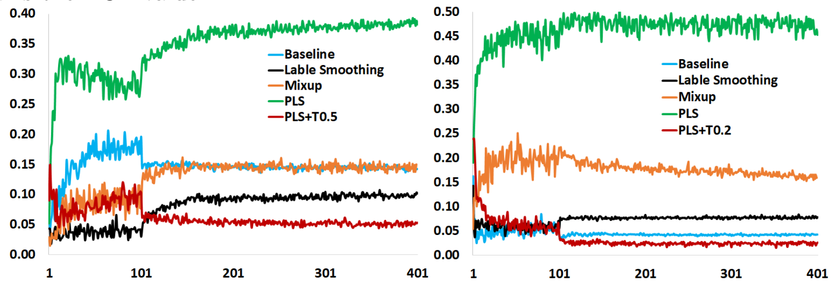

and then let the trained networks to predict on the testing samples from the SVHN dataset (i.e., out-of-distribution samples). We compare our method with the vanilla baseline (ResNet-18 or ResNet-50), Mixup, and ULS-0.1. The winning predicted softmax scores on the SVHN testing samples are presented in Figure 7, where the top and bottom rows depict the results for ResNet-18 and ResNet-50, respectively.

Figure 7 shows that, PLS again produces low winning predicted softmax scores (namely less confident) against the samples from the SVHN dataset when training with either Cifar10 or Cifar100 data, when compared to Mixup, ULS, and the vanilla models. For example, when being trained with Cifar10 and tested on the SVHN data with ResNet-18 (the top-left subfigure), PLS produced (orange curve) a spike of score distribution near the midpoint 0.5, with extremely spare distribution in the regions of high confidence. In contrast, while Mixup and ULS (yellow/green curves) are more conservative than the vanilla model on out-of-distribution data, it is noticeably more overconfident than the PLS strategy by producing a spike of prediction with 90% confidence at the right end of the figure.

5 Conclusion and Future Work

We proposed a novel output distribution regularization technique, coined PLS, which learns smoothing distribution for midpoint samples that average random sample pairs. We empirically showed PLS' superior accuracy over label smoothing and Mixup models. We visualized the high uncertainty training labels of the midpoint samples, which cause PLS to produce very low winning softmax scores for unseen in and out of distribution samples.

Our studies here suggest some interesting directions for future investigation. For example, what are the other benefits arising from high uncertainty training labels and conservative classification? Would such uncertain predictions help with beam search or ranking process for some downstream applications? Does the proposed method benefit from mixing more than two samples for smoothing?

Fig. 7. Winning softmax scores produced by PLS, Mixup, ULS, and baseline models, when being trained with Cifar10 (left) and Cifar100 (right) and then testing on SVHN with PreAct ResNet-18 (top) and ResNet-50 (bottom).

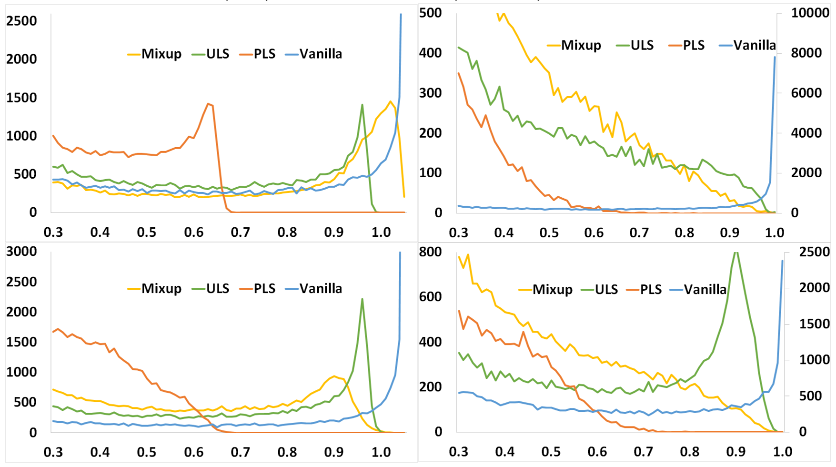

Another interesting research direction would be providing theoretical explanation on why the method works considering that the synthetic images are not realistic. We are also interested in applying our strategy to other domains beyond image.

References

1. Ahn, S., Hu, S.X., Damianou, A., Lawrence, N.D., Dai, Z.: Variational information distillation for knowledge transfer. In: arXiv (2019)
2. Archambault, G.P., Mao, Y., Guo, H., Zhang, R.: Mixup as directional adversarial training. vol. abs/1906.06875 (2019)
3. Carratino, L., Cissé, M., Jenatton, R., Vert, J.P.: On mixup regularization. In: arXiv (2020)
4. Chorowski, J., Jaitly, N.: Towards better decoding and language model integration in sequence to sequence models. In: INTERSPEECH (2016)
5. Chrabaszcz, P., Loshchilov, I., Hutter, F.: A downsampled variant of imagenet as an alternative to the CIFAR datasets. In: arXiv (2017)
6. Furlanello, T., Lipton, Z.C., Tschannen, M., Itti, L., Anandkumar, A.: Born again neural networks. In: ICML (2018)
7. Guo, C., Pleiss, G., Sun, Y., Weinberger, K.Q.: On calibration of modern neural networks. In: ICML. ICML'17, JMLR.org (2017)
8. Guo, H.: Nonlinear mixup: Out-of-manifold data augmentation for text classification. In: AAAI. pp. 4044–4051 (2020)
9. Guo, H., Mao, Y., Zhang, R.: Augmenting data with mixup for sentence classification: An empirical study. vol. abs/1905.08941 (2019)
10. Guo, H., Mao, Y., Zhang, R.: Mixup as locally linear out-of-manifold regularization. In: AAAI. pp. 3714–3722 (2019)

11. He, K., Zhang, X., Ren, S., Sun, J.: Identity mappings in deep residual networks. ECCV (2016)
12. Hinton, G., Vinyals, O., Dean, J.: Distilling the knowledge in a neural network. In: arXiv (2015)
13. Huang, Y., Cheng, Y., Chen, D., Lee, H., Ngiam, J., Le, Q.V., Chen, Z.: Gpipe: Efficient training of giant neural networks using pipeline parallelism. In: NeurIPS (2019)
14. Ioffe, S.: Batch renormalization: Towards reducing minibatch dependence in batch-normalized models. In: Guyon, I., von Luxburg, U., Bengio, S., Wallach, H.M., Fergus, R., Vishwanathan, S.V.N., Garnett, R. (eds.) NeurIPS. pp. 1945–1953 (2017)
15. Li, W., Dasarathy, G., Berisha, V.: Regularization via structural label smoothing. In: AISTAT (2020)
16. Lukasik, M., Bhojanapalli, S., Menon, A.K., Kumar, S.: Does label smoothing mitigate label noise? ICML (2020)
17. Mobahi, H., Farajtabar, M., Bartlett, P.L.: Self-distillation amplifies regularization in hilbert space. In: arXiv (2020)
18. Müller, R., Kornblith, S., Hinton, G.E.: When does label smoothing help? In: NIPS (2019)
19. Pereyra, G., Tucker, G., Chorowski, J., Kaiser, L., Hinton, G.E.: Regularizing neural networks by penalizing confident output distributions. In: ICLR workshop (2017)
20. Real, E., Aggarwal, A., Huang, Y., Le, Q.V.: Regularized evolution for image classifier architecture search. In: AAAI (2019)
21. Szegedy, C., Vanhoucke, V., Ioffe, S., Shlens, J., Wojna, Z.: Rethinking the inception architecture for computer vision. 2016 IEEE Conference on Computer Vision and Pattern Recognition (CVPR) pp. 2818–2826 (2016)
22. Tokozume, Y., Ushiku, Y., Harada, T.: Learning from between-class examples for deep sound recognition. In: ICLR (2018)
23. Vaswani, A., Shazeer, N., Parmar, N., Uszkoreit, J., Jones, L., Gomez, A.N., Kaiser, L., Polosukhin, I.: Attention is all you need. ArXiv **abs/1706.03762** (2017)
24. Xie, L., Wang, J., Wei, Z., Wang, M., Tian, Q.: Disturblabel: Regularizing cnn on the loss layer. In: 2016 IEEE Conference on Computer Vision and Pattern Recognition (CVPR). pp. 4753–4762 (2016)
25. Yang, C., Xie, L., Qiao, S., Yuille, A.L.: Training deep neural networks in generations: A more tolerant teacher educates better students. In: AAAI. pp. 5628–5635. AAAI Press (2019)
26. Yuan, L., Tay, F.E.H., Li, G., Wang, T., Feng, J.: Revisit knowledge distillation: a teacher-free framework. In: arXiv (2019)
27. Yun, S., Han, D., Chun, S., Oh, S.J., Yoo, Y., Choe, J.: Cutmix: Regularization strategy to train strong classifiers with localizable features. In: ICCV. pp. 6022–6031. IEEE (2019)
28. Zhang, H., Cissé, M., Dauphin, Y.N., Lopez-Paz, D.: mixup: Beyond empirical risk minimization. In: ICLR (2018)
29. Zhu, Z., Jiang, X., Zheng, F., Guo, X., Huang, F., Sun, X., Zheng, W.: Viewpoint-aware loss with angular regularization for person re-identification. In: AAAI. pp. 13114–13121 (2020)
30. Zoph, B., Vasudevan, V., Shlens, J., Le, Q.V.: Learning transferable architectures for scalable image recognition. In: 2018 IEEE/CVF Conference on Computer Vision and Pattern Recognition. pp. 8697–8710 (2018)